

Analytic solutions for the static equilibrium configurations of externally loaded cantilever soft robotic arms

Stanislao Grazioso¹, Giuseppe Di Gironimo¹ and Bruno Siciliano²

Abstract—In this paper we derive the analytic solutions for the statics of cantilever soft arm under external loading. The main motivation behind this work is the development of manageable and ready-to-use mathematical models of soft robotic arm for various purposes. We formulate the problem exploiting the Lie group structure of the arms' configuration space. This allows using the powerful mathematical tools from differential geometry. The model builds upon the theory of Cosserat rods: the mechanics-based perspective used to describe the kinematics and statics allows including into the model the large deformations due to axial, shear, torsion and bending effects. The position fields of the manipulators' shapes are analytically integrated and validated with respect to exact solutions and experiments.

Index Terms—Soft robotics, differential geometry, Cosserat rods, mathematical modeling.

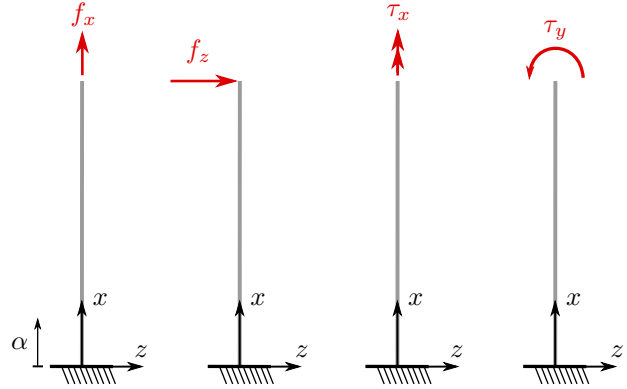


Fig. 1. Externally loaded cantilever soft arm.

NOMENCLATURE

$\dot{(\cdot)}$	derivative with respect to time
$(\cdot)'$	derivative with respect to space
$\widetilde{(\cdot)}$	$\mathbb{R}^6 \rightarrow \mathfrak{se}(3)$
(\cdot, \cdot)	$\mathfrak{se}(3) \times \mathfrak{se}(3) \rightarrow \mathfrak{se}(3)$
$\widehat{(\cdot)}$	$\mathbb{R}^6 \rightarrow \mathbb{R}^{6 \times 6}$
t	$\in \mathbb{R}$, time
α	$\in \mathbb{R}$, reference curve parametrization
\mathbf{u}	$\in \mathbb{R}^3$, position vector
\mathbf{R}	$\in SO(3)$, rotation matrix
\mathbf{H}	$\in SE(3)$, configuration matrix
$\boldsymbol{\eta}$	$\in \mathbb{R}^6$, velocity vector
\mathbf{f}	$\in \mathbb{R}^6$ deformation vector
$\boldsymbol{\sigma}$	$\in \mathbb{R}^6$, stress vector

I. INTRODUCTION

Modeling of soft robotic arms has shown significant advancements over the last few years, and many mathematical formulations have been proposed [1]. Currently, the most adopted kinematic modeling methods involve a *discrete* or *constant-curvature* approximation. The first one discretizes a continuous elastic structure through a series of rigid links connected by conventional revolute, universal, or spherical

joints [2]. The second one represents a continuum robot geometry with a finite collection of circular arcs, which are defined by only three parameters, namely radius of curvature, angle of the arc and bending plane [3]. More accurate results can be achieved with a *variable-curvature* approach [4]. It typically adopts a material-attached homogeneous reference frame comprising a position vector $\mathbf{u}(\alpha) \in \mathbb{R}^3$ and a rotation matrix $\mathbf{R}(\alpha) \in SO(3)$, and expresses the arm pose as a function of the material abscissa along the robot. On the top of kinematics, *lumped-parameters* [5] or more accurate *distributed-parameters* [6], [7], [8] models can be used to derive mechanics-based representations of the governing equations for the robot's shape. The latter models typically involve classical elasticity theories from continuum mechanics, including Euler-Bernoulli, Timoshenko, Kirchoff and Cosserat beams [9], [10], [11].

However, the high complexity of these models, and the associated tedious computer implementation, make their use still limited. For accurate computer simulation of such mechanical systems, the current practice is still to use classical nonlinear finite element solvers [12]. The main problem of a numerical approach is that it can be used only for simulation, since it complicates the derivation of model-based control and planning algorithms. Therefore, the development of manageable and potentially useful analytical solutions for practical problems in soft robotics is highly desirable.

In this paper we derive analytic solutions for the statics of cantilever soft robotic arms subject to end loads. Many practical systems can be modeled as cantilever arms, such as soft actuators for whole-body manipulation [13], which recently have been used as wearable systems for robotic rehabilitation [14] [15].

¹ Stanislao Grazioso and Giuseppe Di Gironimo are with the Department of Industrial Engineering, University of Naples Federico II and CREATE Consortium, 80125, Napoli, Italy, {stanislao.grazioso, giuseppe.digironimo}@unina.it

² Bruno Siciliano is with PRISMA Lab, Department of Electrical Engineering and Information Technology, University of Naples Federico II and CREATE Consortium, 80125, Napoli, Italy, bruno.siciliano@unina.it

We model a soft robotic arm as a beam defined by a continuous assembly of rigid cross-sections subject to transformations along a three-dimensional curve. We define the position and orientation fields of the arm on a Lie group, the special Euclidean group $SE(3)$ [16], [17]. After, we define the velocity and deformation fields respectively from the time and space derivatives on $SE(3)$. A material constitutive law between internal forces and internal deformations allows defining the internal strain energy of the arm. Therefore, we apply the principle of virtual work to derive the static equilibrium equations. We analytically integrate these equations for the cantilever arms analyzed in this paper. Finally, we validate the achieved closed-form solutions with respect to exact solutions and experiments. Basic operations on Lie groups are reported in Appendix.

II. KINEMATICS

The position field, which describes the configuration of the soft arm, is represented by the mapping

$$\alpha \in \mathbb{R} \mapsto \mathbf{H}(\alpha) = \mathcal{H}(\mathbf{R}(\alpha), \mathbf{u}(\alpha)) \in SE(3) \quad (1)$$

where $\alpha \in [0, L]$ is the material abscissa which parametrizes the reference curve of the soft arm with length L .

The deformation field is defined from the space derivative of the position field. According to the definition of derivatives on $SE(3)$ (see, e.g. Eq. 61), an element $\tilde{\mathbf{f}}(\alpha) \in \mathfrak{se}(3)$, representing the deformation measures, can be introduced as

$$\mathbf{H}'(\alpha) = \mathbf{H}(\alpha)\tilde{\mathbf{f}}(\alpha). \quad (2)$$

The deformation measures are defined from the initial configuration as

$$\mathbf{f}(\alpha) = \mathbf{f}^0 + \boldsymbol{\epsilon}(\alpha) \quad (3)$$

where \mathbf{f}^0 is the initial deformation vector and $\boldsymbol{\epsilon}(\alpha)$ is the 6×1 strain vector which includes the classical position part and orientation part of the deformations as

$$\boldsymbol{\epsilon}(\alpha) = \begin{bmatrix} \boldsymbol{\gamma}(\alpha) \\ \boldsymbol{\kappa}(\alpha) \end{bmatrix} \quad (4)$$

where $\boldsymbol{\gamma}(\alpha)$ includes the axial and the two shear deformations, while $\boldsymbol{\kappa}(\alpha)$ includes the torsional and the two bending deformations. In the same way, the velocity field is obtained by taking the time derivatives of the position field. By using again the representation of the derivatives on $SE(3)$, the velocity variables are introduced as an element $\tilde{\boldsymbol{\eta}}(\alpha) \in \mathfrak{se}(3)$, which is associated to the 6×1 axial vector

$$\boldsymbol{\eta}(\alpha) = \begin{bmatrix} \mathbf{v}(\alpha) \\ \boldsymbol{\omega}(\alpha) \end{bmatrix} \quad (5)$$

where $\mathbf{v}(\alpha)$ and $\boldsymbol{\omega}(\alpha)$ are respectively the linear and angular velocities. Hence, the derivative of (1) with respect to time yields

$$\dot{\mathbf{H}}(\alpha) = \mathbf{H}(\alpha)\tilde{\boldsymbol{\eta}}(\alpha) \quad (6)$$

which constitutes the velocity field of a soft continuum arm.

III. STATICS

The static equilibrium equations are obtained by applying the principle of virtual work, after having defined the internal strain energy of the soft arm.

A. Strain energy

The internal strain energy is defined as

$$\mathcal{V}_{int} = \frac{1}{2} \int_L \boldsymbol{\epsilon}^T \boldsymbol{\sigma} d\alpha \quad (7)$$

where

$$\boldsymbol{\sigma}(\alpha) = \begin{bmatrix} \mathbf{n}(\alpha) \\ \mathbf{m}(\alpha) \end{bmatrix} \quad (8)$$

is the vector of the stress resultants over the cross-section of the arm, and \mathbf{n} and \mathbf{m} are the 3×1 resulting force and resulting moment vectors. In particular, n_1 is the force along the reference curve, while n_2 and n_3 are the shear forces along the cross-section axes. Indeed, m_1 is the torsion moment about the reference curve, while m_2 and m_3 are the bending moments about the cross-section axes.

The internal forces $\boldsymbol{\sigma}$ and the mechanical strains $\boldsymbol{\epsilon}$ can be related through the material constitutive law. Linear constitutive equations for an isotropic elastic material lead to

$$\mathbf{r} = \mathbf{K}\boldsymbol{\epsilon} \quad (9)$$

where \mathbf{K} is the 6×6 stiffness matrix given by

$$\mathbf{K} = \begin{bmatrix} \mathbf{K}_{uu} & \mathbf{K}_{u\omega} \\ \text{SYM} & \mathbf{K}_{\omega\omega} \end{bmatrix} \quad (10)$$

In general, the stiffness matrix is not diagonal. In case of an initially straight configuration of the soft arm, it becomes diagonal when the reference curve is chosen to be the neutral axis of the arm, and the normal and the bi-normal to the curve are chosen to be the principal axes of the cross-sections. In such case,

$$\mathbf{K}_{uu} = \text{diag}(EA, GA_y, GA_z) \quad (11)$$

contains the axial and shear stiffnesses, while

$$\mathbf{K}_{\omega\omega} = \text{diag}(GJ, EI_y, EI_z) \quad (12)$$

contains the torsional and bending stiffnesses. In (11) and (12), E and $G \in \mathbb{R}$ denote respectively the Young and the shear modulus. For an isotropic material, it holds $G = E/2(1 + \nu)$, where $\nu \in \mathbb{R}$ is the Poisson ratio. Using (9), Eq. (7) becomes

$$\mathcal{V}_{int} = \frac{1}{2} \int_L \boldsymbol{\epsilon}^T \mathbf{K}\boldsymbol{\epsilon} d\alpha \quad (13)$$

where we can recognize the well known structure of the internal energy for a linear elastic material expressed as a quadratic form in $\boldsymbol{\epsilon}$.

B. Static equilibrium equations

According to the principle of virtual work, the manipulator is in static equilibrium if and only if

$$\delta(\mathcal{V}_{int}) = \delta(\mathcal{V}_{ext}) \quad (14)$$

where $\delta(\mathcal{V}_{ext})$ is the virtual work done by the external forces. The variation of the expression of the internal energy in (7) reads

$$\delta(\mathcal{V}_{int}) = \int_L \delta(\boldsymbol{\epsilon})^T \boldsymbol{\sigma} d\alpha \quad (15)$$

where, recalling the commutativity of the Lie derivatives in (66), the variation of the strains can be expressed as

$$\delta(\boldsymbol{\epsilon}) = \delta(\mathbf{f}) = (\delta\mathbf{h})' + \widehat{\mathbf{f}}\delta\mathbf{h} \quad (16)$$

in which we used $\delta(\mathbf{H}(\alpha)) = \mathbf{H}(\alpha)\widehat{\delta\mathbf{h}}(\alpha)$. Inserting (16) into (15) and integrating by parts yield

$$\delta(\mathcal{V}_{int}) = \left[\delta\mathbf{h}^T \boldsymbol{\sigma} \right] \Big|_0^L - \int_L \delta\mathbf{h}^T (\boldsymbol{\sigma}' - \widehat{\mathbf{f}}^T \boldsymbol{\sigma}) d\alpha \quad (17)$$

where the first term at the right hand side is interpreted as a boundary condition.

In general, the virtual work done by the external forces can be expressed as

$$\delta(\mathcal{V}_{ext}) = \delta\mathbf{h}(0)^T \mathbf{g}_{ext}(0) - \delta\mathbf{h}(L)^T \mathbf{g}_{ext}(L) - \int_L \delta\mathbf{h}^T \mathbf{g}_{ext} d\alpha \quad (18)$$

where $\mathbf{g}_{ext}(\alpha) = [\mathbf{g}_{ext,u}^T \ \mathbf{g}_{ext,\omega}^T]^T$ contains the resulting forces and moments over the cross-sections due to the external loading.

Finally, the weak form of the static equilibrium equations is obtained by inserting (18) and (17) into (14), which yields

$$\left[\delta\mathbf{h}^T (\boldsymbol{\sigma} - \mathbf{g}_{ext}) \right] \Big|_0^L - \int_L \delta\mathbf{h}^T (\boldsymbol{\sigma}' - \widehat{\mathbf{f}}^T \boldsymbol{\sigma} - \mathbf{g}_{ext}) d\alpha = 0 \quad (19)$$

Indeed, the strong form reads

$$\boldsymbol{\sigma}' - \widehat{\mathbf{f}}^T \boldsymbol{\sigma} = \mathbf{g}_{ext} \quad (20)$$

which constitute the Reissner equations for the static case.

IV. ANALYTIC SOLUTIONS

In this section we derive the closed-form analytic solutions for the steady-state statics of cantilever soft arm subject to external moments and forces.

A. External moments

External moments applied at the free end of cantilever soft arms about the neutral axis or the cross-section axes induce pure torsion/bending solicitations (see, e.g., Fig. 1). Since the arms are clamped in the origin, we have that $\delta\mathbf{h}(0) = \mathbf{0}_{6 \times 1}$, while the boundary conditions in the free end are

$$\boldsymbol{\sigma}(L) = \mathbf{K}(L)\boldsymbol{\epsilon}(L) = \mathbf{g}_{ext} \quad (21)$$

where we consider the soft arm made of linear elastic material. Moreover, we consider constant cross-section properties and constant initial curvature and torsion of the reference curve. Under these hypothesis, \mathbf{f}^0 and \mathbf{K} are constant over the length of the arm.

1) *Deformation field*: The equilibrium equations in the static configuration expressed by (20) become

$$\mathbf{K}\boldsymbol{\epsilon}' - \widehat{\mathbf{f}}^0 \mathbf{K}\boldsymbol{\epsilon} = \mathbf{0}_{6 \times 1} \quad (22)$$

where we used the fact that the stiffness matrix is constant over the arm. In this case, the solution for the deformation field can be expressed in closed form and it is given by

$$\boldsymbol{\epsilon}(\alpha) = \mathbf{K}^{-1} \mathbf{F}(\alpha) \mathbf{K} \boldsymbol{\epsilon}_0 \quad (23)$$

where $\boldsymbol{\epsilon}_0$, the deformation at $\alpha = 0$, is a constant of integration and

$$\mathbf{F}(\alpha) = \begin{bmatrix} \mathbf{L}^T(\alpha) & \mathbf{0}_{3 \times 3} \\ (\mathbf{T}_{SO(3)}(\alpha \mathbf{f}_\omega^0) \alpha \mathbf{f}_u^0)^{\sim} \mathbf{L}^T(\alpha) & \mathbf{L}^T(\alpha) \end{bmatrix} \quad (24)$$

with $\mathbf{L}(\alpha) = \exp_{SO(3)}(\alpha \mathbf{f}_\omega^0)$. Notice that we indicate the position part of the deformation with \mathbf{f}_u , while the orientation part with \mathbf{f}_ω . Indeed, the tangent operator $\mathbf{T}_{SO(3)}(\cdot)$ is given in (73). Inserting (23), computed at $\alpha = L$, in the boundary condition given by (21), yields

$$\boldsymbol{\sigma}(L) = \mathbf{K} \mathbf{K}^{-1} \mathbf{F}(L) \mathbf{K} \boldsymbol{\epsilon}_0 = \mathbf{g}_{ext}(L) \quad (25)$$

such that the constant of integration $\boldsymbol{\epsilon}_0$ is given by

$$\boldsymbol{\epsilon}_0 = \mathbf{K}^{-1} (\mathbf{F}(L))^{-1} \mathbf{g}_{ext}(L) \quad (26)$$

Therefore, by introducing (26) in (23), the solution for the deformation field reads

$$\boldsymbol{\epsilon}(\alpha) = \mathbf{K}^{-1} \mathbf{F}(\alpha) (\mathbf{F}(L))^{-1} \mathbf{g}_{ext}(L) \quad (27)$$

In the special cases of pure bending/torsion solicitations, the external forces are given by

$$\mathbf{g}_{ext,u}(L) = \mathbf{0}_{3 \times 1} \quad (28)$$

$$\mathbf{g}_{ext,\omega}(L) = \tau \mathbf{a} \quad (29)$$

where $\tau \in \mathbb{R}$ and $\mathbf{a} \in \mathbb{R}^3$ is an arbitrary vector. For an initially straight arm, we have $\mathbf{F}(\alpha) (\mathbf{F}(L))^{-1} = \mathbf{I}_{6 \times 6}$. Hence, the deformation field in (27) becomes

$$\boldsymbol{\epsilon} = \mathbf{K}^{-1} \begin{bmatrix} \mathbf{0}_{3 \times 1} \\ \tau \mathbf{a} \end{bmatrix} \quad (30)$$

Thus, it results that $\boldsymbol{\epsilon}$ is constant along the continuum arm. By separating the position and the orientation parts of the strains, the solution reads

$$\begin{bmatrix} \boldsymbol{\gamma} \\ \boldsymbol{\kappa} \end{bmatrix} = \begin{bmatrix} \mathbf{0}_{3 \times 1} \\ \mathbf{K}_{\omega\omega}^{-1}(\tau \mathbf{a}) \end{bmatrix} \quad (31)$$

where $\mathbf{K}_{\omega\omega}$ is given in (12).

2) *SE(3) field*: The position and orientation fields are obtained by solving the kinematic equations in (2). Since the deformation field obtained above in (30) involves constant strains, Eq. 2 can be integrated analytically and the solution for the *SE(3)* field is given by

$$\mathbf{H}(\alpha) = \mathbf{H}_0 \exp_{SE(3)}(\alpha (\mathbf{f}^0 + \boldsymbol{\epsilon})) \quad (32)$$

where $\mathbf{H}_0 = \mathcal{H}(\mathbf{R}_0, \mathbf{u}_0)$ is a constant of integration and $\exp_{SE(3)}(\cdot)$ is the exponential map on *SE(3)* given by (69). Explicitly, Eq. (32) means

$$\mathbf{u}(\alpha) = \mathbf{u}_0 + \mathbf{R}_0 \mathbf{T}_{SO(3)}^T(\alpha (\mathbf{f}_\omega^0 + \boldsymbol{\kappa})) \alpha (\mathbf{f}_u^0 + \boldsymbol{\gamma}) \quad (33)$$

$$\mathbf{R}(\alpha) = \mathbf{R}_0 \exp_{SO(3)}(\alpha (\mathbf{f}_\omega^0 + \boldsymbol{\kappa})) \quad (34)$$

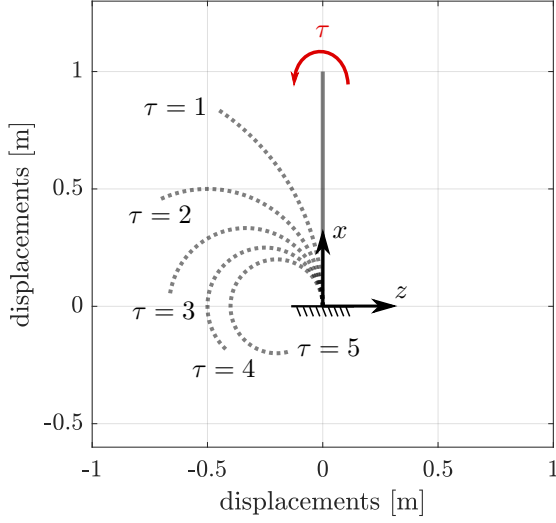


Fig. 2. Static configurations of a cantilever soft arm in pure bending.

Since we are considering initially straight arm, we have that $\mathbf{u}_0 = \mathbf{0}_{3 \times 1}$, $\mathbf{R}_0 = \mathbf{I}_{3 \times 3}$ and $\mathbf{f}_u^0 = [1 \ 0 \ 0]^T$, $\mathbf{f}_\omega^0 = \mathbf{0}_{3 \times 1}$. As illustrative example, let us consider a pure bending tip load as $\mathbf{g}_{ext,\omega}(L) = \tau[0 \ 1 \ 0]^T$. According to (31), the deformations are given by

$$\boldsymbol{\gamma} = [0 \ 0 \ 0]^T \quad (35)$$

$$\boldsymbol{\kappa} = [0 \ \kappa_y \ 0]^T \quad (36)$$

where $\kappa_y = \tau/(EI_y)$. Indeed, according to (33)–(34), the position and rotation fields are given by

$$\mathbf{u}(\alpha) = \begin{bmatrix} \frac{1}{\kappa_y} \sin(\alpha \kappa_y) \\ 0 \\ -\frac{1}{\kappa_y} (1 - \cos(\alpha \kappa_y)) \end{bmatrix} \quad (37)$$

$$\mathbf{R}(\alpha) = \begin{bmatrix} \cos(\alpha \kappa_y) & 0 & \sin(\alpha \kappa_y) \\ 0 & 1 & 0 \\ -\sin(\alpha \kappa_y) & 0 & \cos(\alpha \kappa_y) \end{bmatrix} \quad (38)$$

which is the exact solution known since Euler, i.e. the solution for the position field of a cantilever soft arm in pure bending and large displacements is a circle of radius $\rho = 1/\kappa_y$ [18]. By considering $EI_y = 1 \text{ Nm}^2$ and $L = 1 \text{ m}$, the soft arm's steady-state shape, for bending tip loads $\tau = 1, 2, 3, 4, 5 \text{ N m}$, is given in Fig. 2. The other two cases are obtained in the same manner.

B. External forces

An external force applied at the free end of a cantilever soft arm along the neutral axis induces a constant axial deformation given by $\boldsymbol{\gamma} = [F/EA \ 0 \ 0]^T$, being F the axial force. The position field is then obtained using (32). Indeed, a shear force along one of the cross-section axes involves a more complex problem, described as follows. Let us consider an end force $\mathbf{P} = [0 \ 0 \ P]^T$. Since the arm is clamped in the origin, we have again that $\delta \mathbf{h}(0) = \mathbf{0}_{6 \times 1}$, while the boundary conditions in the free end are again given by (21),

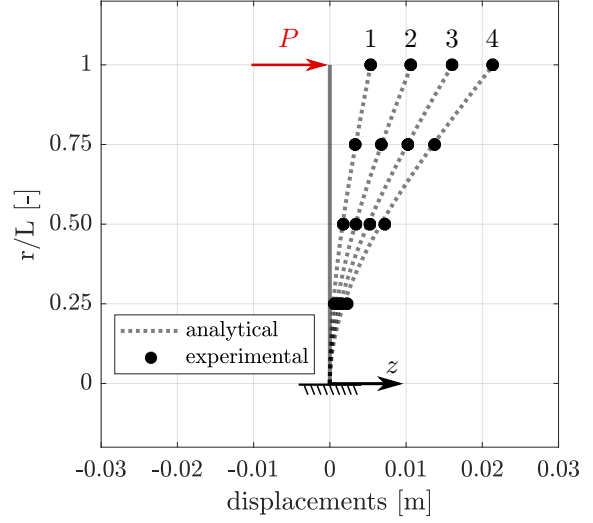


Fig. 3. Static configurations of a cantilever soft arm with a shear load.

since we consider the soft arm made of linear elastic material. By splitting the position and orientation part, we obtain

$$\mathbf{K}_{uu} \boldsymbol{\gamma}(L) = \mathbf{P} \quad (39)$$

$$\mathbf{K}_{\omega\omega} \boldsymbol{\kappa}(L) = \mathbf{0}_{3 \times 1} \quad (40)$$

Furthermore, we consider constant cross-section properties and initially straight configuration of the arm. Under these hypothesis, \mathbf{K} is constant over the length of the arm, while $\mathbf{f}_\omega^0 = \mathbf{0}_{3 \times 1}$ and $\mathbf{f}_u^0 = [1 \ 0 \ 0]^T$, since the arm is aligned along \mathbf{x} .

1) *Deformation field:* The equilibrium equations in the static configuration expressed by (20) become

$$\mathbf{K}_{uu} \boldsymbol{\gamma}' = \mathbf{0}_{3 \times 1} \quad (41)$$

$$\mathbf{K}_{\omega\omega} \boldsymbol{\kappa}' - \tilde{\mathbf{f}}_u^0 \mathbf{K}_{uu} \boldsymbol{\gamma} = \mathbf{0}_{3 \times 1} \quad (42)$$

The solution of (41)–(42) can be expressed as

$$\boldsymbol{\gamma} = \mathbf{c}_1 \quad (43)$$

$$\boldsymbol{\kappa}(\alpha) = -(\mathbf{K}_{\omega\omega}^{-1} \tilde{\mathbf{f}}_u^0 \mathbf{K}_{uu} \mathbf{c}_1) \alpha + \mathbf{c}_2 \quad (44)$$

where \mathbf{c}_1 and \mathbf{c}_2 are two constants of integration. They can be determined from the boudary conditions (39)–(40) as

$$\mathbf{K}_{uu} \mathbf{c}_1 = \mathbf{P} \quad (45)$$

$$\mathbf{K}_{\omega\omega} (-(\mathbf{K}_{\omega\omega}^{-1} \tilde{\mathbf{f}}_u^0 \mathbf{K}_{uu} \mathbf{c}_1) L + \mathbf{c}_2) = \mathbf{0}_{3 \times 1} \quad (46)$$

giving the solutions

$$\mathbf{c}_1 = \mathbf{K}_{uu}^{-1} \mathbf{P} = \begin{bmatrix} 0 & 0 & \frac{P}{GA_z} \end{bmatrix}^T \quad (47)$$

$$\mathbf{c}_2 = -L \mathbf{K}_{\omega\omega}^{-1} \tilde{\mathbf{f}}_u^0 \mathbf{K}_{uu} \mathbf{c}_1 = \begin{bmatrix} 0 & -\frac{LP}{EI_y} & 0 \end{bmatrix}^T \quad (48)$$

Hence, the analytic solutions for the deformation field read

$$\boldsymbol{\gamma} = \begin{bmatrix} 0 & 0 & \frac{P}{GA_z} \end{bmatrix}^T \quad (49)$$

$$\boldsymbol{\kappa}(\alpha) = \begin{bmatrix} 0 & -\frac{LP}{EI_y} \left(\frac{\alpha}{L} - 1 \right) & 0 \end{bmatrix}^T \quad (50)$$

which involve a constant shear strain and a variable bending strain along the length of the arm.

2) *SE(3) field*: The configuration of the soft arm is obtained by integrating (2). In this example, the position and orientation parts of (2) read

$$\mathbf{u}'(\alpha) = \mathbf{R}(\alpha)(\mathbf{f}_u^0 + \boldsymbol{\gamma}) \quad (51)$$

$$\mathbf{R}'(\alpha) = \mathbf{R}(\alpha)\tilde{\boldsymbol{\kappa}}(\alpha) \quad (52)$$

In order to integrate analytically (51)–(52) which involve a variable deformation, we need to assume small displacements for the *SE(3)* field. Accordingly, the rotation matrix and its derivative read

$$\mathbf{R}(\alpha) = \mathbf{I}_{3 \times 3} + \tilde{\boldsymbol{\theta}}(\alpha) \quad \mathbf{R}'(\alpha) = \tilde{\boldsymbol{\theta}}'(\alpha) \quad (53)$$

where $\boldsymbol{\theta}(\alpha) = [0 \ \theta(\alpha) \ 0]^T$ since the motion is planar. By introducing (53) into (51)–(52), we obtain

$$\mathbf{u}'(\alpha) = \mathbf{f}_u^0 + \boldsymbol{\gamma} - \tilde{\mathbf{f}}_u^0 \boldsymbol{\theta}(\alpha) \quad (54)$$

$$\boldsymbol{\theta}'(\alpha) = \boldsymbol{\kappa}(\alpha) \quad (55)$$

The integration of Eqs. 54–55 is given by

$$\begin{aligned} \mathbf{u}(\alpha) &= (\mathbf{f}_u^0 + \boldsymbol{\gamma})\alpha + \dots \\ &\dots - \tilde{\mathbf{f}}_u^0 \left(-(\mathbf{K}_{\omega\omega}^{-1} \tilde{\mathbf{f}}_u^0 \mathbf{K}_{uu} \mathbf{c}_1) \frac{\alpha^3}{6} + \mathbf{c}_2 \frac{\alpha^2}{2} \right) + \mathbf{c}_4 \end{aligned} \quad (56)$$

$$\boldsymbol{\theta}(\alpha) = -(\mathbf{K}_{\omega\omega}^{-1} \tilde{\mathbf{f}}_u^0 \mathbf{K}_{uu} \mathbf{c}_1) \frac{\alpha^2}{2} + \mathbf{c}_2 \alpha + \mathbf{c}_3 \quad (57)$$

where the boundary conditions $\mathbf{u}(0) = \mathbf{0}$ and $\boldsymbol{\theta}(0) = \mathbf{0}$ yield $\mathbf{c}_3 = \mathbf{0}$ and $\mathbf{c}_4 = \mathbf{0}$. Hence, using (47)–(48), the configuration of the soft arm reads

$$\mathbf{u}(\alpha) = \begin{bmatrix} \alpha \\ 0 \\ \alpha \frac{P}{GA_z} + \frac{PL^3}{6EI_y} \left(\frac{3\alpha^2}{L^2} - \frac{\alpha^3}{L^3} \right) \end{bmatrix} \quad (58)$$

$$\boldsymbol{\theta}(\alpha) = \begin{bmatrix} 0 \\ -\frac{PL^2}{EI_y} \left(\frac{\alpha}{L} - \frac{\alpha^2}{2L^2} \right) \\ 0 \end{bmatrix} \quad (59)$$

In order to validate the model, let us consider the experimental study in [19], where the elastic arm subject to a shear force has the following properties: $EI_y = 36.28 \text{ Nm}^2$, $GA_z = 0.9039 \times 10^6 \text{ Nm}^2$ and $L = 0.508 \text{ m}$. Figure 3 shows the displacements along the z -direction of the arm, when subject to four loading conditions: $P_1 = 4.448 \text{ N}$, $P_2 = 8.896 \text{ N}$, $P_3 = 13.345 \text{ N}$, $P_4 = 17.792 \text{ N}$. A close agreement of the analytic solution with the experimental deflections is observed. For a more detailed analysis, we define a percentage error measure $e[\%]$ as

$$e[\%] = \frac{z - z_e}{r/L} \cdot 100 \quad (60)$$

where z is the third component of the displacements computed according to (58), z_e is the experimental displacement and r/L is the radial station along the arm's length.

TABLE I
PERCENTAGE ERRORS OF THE SHEAR LOAD PROBLEM

r/L	P_1	P_2	P_3	P_4
0.25	0.049	0.078	0.056	0.166
0.50	0.015	0.016	0.046	0.102
0.75	0.008	0.004	0.008	0.023
1	< 0.001	0.001	0.005	0.008

Table I reports the percentage errors for all the loading conditions of this problem. Even if the errors slightly increase by increasing the shear force, they are all far below 1%.

V. CONCLUSIONS

In this paper analytic models for the kinematics and the statics of externally loaded cantilever soft arms were derived. We approached the problem exploiting the Lie group structure of the configuration space, and we used the powerful mathematical tools from differential geometry. The models derive from the Cosserat rod theory, and they account for the large deformations due to elongation, shear, torsion and bending. The results shows that this approach leads to the exact solution for arms in pure bending. Indeed, the percentage errors of the analytic deflections, with respect to the experimental deflections, when the arm is subject to a shear force, are below 1%.

The availability of ready-to-use mathematical models could be fundamental in designing efficient model-based controllers and planning algorithms for practical and usual problems in the emerging field of soft robotics.

APPENDIX

This Appendix reports some basic operations on a Lie group.

A. Lie derivative

Given $a \in \mathbb{R}$ and $\mathbf{H} \in SE(3)$, the Lie derivative of \mathbf{H} with respect to α reads

$$d_\alpha(\mathbf{H}) = \mathbf{H}\tilde{\mathbf{h}} \quad (61)$$

where $\tilde{\mathbf{h}} \in \mathfrak{se}(3)$ is an invariant vector field called Lie algebra. The Lie algebra $\mathfrak{se}(3)$ is the space of 4×4 matrices as

$$\tilde{\mathbf{h}} = \begin{bmatrix} \tilde{\mathbf{h}}_\omega & \mathbf{h}_u \\ \mathbf{0}_{1 \times 3} & 0 \end{bmatrix} \quad (62)$$

where

$$\tilde{\mathbf{h}}_\omega = \begin{bmatrix} 0 & -h_{\omega,3} & h_{\omega,2} \\ h_{\omega,3} & 0 & -h_{\omega,1} \\ -h_{\omega,2} & h_{\omega,1} & 0 \end{bmatrix} \quad (63)$$

is the rotational skew-symmetric matrix. The Lie algebra $\tilde{\mathbf{h}} \in \mathfrak{se}(3)$ is isomorphic to \mathbb{R}^6 , with

$$\mathbf{h} = \begin{bmatrix} \mathbf{h}_\omega \\ \mathbf{h}_u \end{bmatrix} \quad (64)$$

where $\mathbf{h}_\omega = [h_{\omega,1} \ h_{\omega,2} \ h_{\omega,3}]^T$ and $\mathbf{h}_u = [h_{u,1} \ h_{u,2} \ h_{u,3}]^T$.

B. Lie bracket

Given $\tilde{\mathbf{h}}_1 \in \mathfrak{se}(3)$ and $\tilde{\mathbf{h}}_2 \in \mathfrak{se}(3)$, defined respectively from the Lie derivative of \mathbf{H} with respect to $a \in \mathbb{R}$ and $b \in \mathbb{R}$, the commutativity of the cross derivatives can be written as

$$d_b(\tilde{\mathbf{h}}_1) - d_a(\tilde{\mathbf{h}}_2) = [\tilde{\mathbf{h}}_1, \tilde{\mathbf{h}}_2] \quad (65)$$

where $[\cdot, \cdot]$ denotes the Lie bracket operator. According to the isomorphism $\mathfrak{se}(3) \simeq \mathbb{R}^6$, Eq. 65 can be expressed in terms of vectors in \mathbb{R}^6 as

$$d_b(\mathbf{h}_1) - d_a(\mathbf{h}_2) = \hat{\mathbf{h}}_1 \mathbf{h}_2 \quad (66)$$

where

$$\hat{\mathbf{h}} = \begin{bmatrix} \tilde{\mathbf{h}}_\omega & \tilde{\mathbf{h}}_u \\ \mathbf{0}_{3 \times 3} & \tilde{\mathbf{h}}_\omega \end{bmatrix} \quad (67)$$

C. Exponential map

Eq. 61 can be seen as a linear differential equation on a Lie group. If \mathbf{h} does not depend on a , the solution is given by

$$\mathbf{H}(a) = \mathbf{H}_0 \exp_{SE(3)}(\mathbf{h}a) \quad (68)$$

where \mathbf{H}_0 is a constant of integration and $\exp_{SE(3)}(\cdot)$ is the exponential map on $SE(3)$ which is given by

$$\exp_{SE(3)}(\mathbf{h}) = \begin{bmatrix} \exp_{SO(3)}(\mathbf{h}_\omega) & \mathbf{T}_{SO(3)}^T(\mathbf{h}_\omega) \mathbf{h}_u \\ \mathbf{0}_{1 \times 3} & 1 \end{bmatrix} \quad (69)$$

The 3×3 upper left block in (69) is the exponential map on the special Orthogonal group $SO(3)$, which is the space of the rotation matrices. It is given by the Rodriguez' formula as

$$\exp_{SO(3)}(\mathbf{h}_\omega) = \mathbf{I}_{3 \times 3} + \alpha(\mathbf{h}_\omega) \tilde{\mathbf{h}}_\omega + \frac{\beta(\mathbf{h}_\omega)}{2} \tilde{\mathbf{h}}_\omega^2 \quad (70)$$

where

$$\alpha(\mathbf{h}_\omega) = \frac{\sin(\|\mathbf{h}_\omega\|)}{\|\mathbf{h}_\omega\|} \quad \beta(\mathbf{h}_\omega) = 2 \frac{1 - \cos(\|\mathbf{h}_\omega\|)}{\|\mathbf{h}_\omega\|^2} \quad (71)$$

Indeed, the 3×1 upper right column vector in (69) contains the tangent operator defined in the next paragraph.

D. Tangent operator

The tangent operator on $SE(3)$ is given by

$$\mathbf{T}_{SE(3)}(\mathbf{h}) = \begin{bmatrix} \mathbf{T}_{SO(3)}(\mathbf{h}_\omega) & \mathbf{T}_{u\omega}(\mathbf{h}_u, \mathbf{h}_\omega) \\ \mathbf{0}_{3 \times 3} & \mathbf{T}_{SO(3)}(\mathbf{h}_\omega) \end{bmatrix} \quad (72)$$

where

$$\mathbf{T}_{SO(3)}(\mathbf{h}_\omega) = \mathbf{I}_{3 \times 3} - \frac{\beta(\mathbf{h}_\omega)}{2} \tilde{\mathbf{h}}_\omega + \frac{1 - \alpha(\mathbf{h}_\omega)}{\|\mathbf{h}_\omega\|^2} \tilde{\mathbf{h}}_\omega^2 \quad (73)$$

is the tangent operator on $SO(3)$ and

$$\begin{aligned} \mathbf{T}_{u\omega}(\mathbf{h}_u, \mathbf{h}_\omega) &= \frac{-\beta}{2} \tilde{\mathbf{h}}_\omega + \frac{1 - \alpha}{\|\mathbf{h}_\omega\|^2} [\mathbf{h}_u, \mathbf{h}_\omega] + \dots \\ &\dots + \frac{\mathbf{h}_\omega^T \mathbf{h}_u}{\|\mathbf{h}_\omega\|^2} \left((\beta - \alpha) \tilde{\mathbf{h}}_\omega + \left(\frac{\beta}{2} - \frac{3(1 - \alpha)}{\|\mathbf{h}_\omega\|^2} \right) \tilde{\mathbf{h}}_\omega^2 \right) \end{aligned} \quad (74)$$

ACKNOWLEDGMENT

This work was partially supported by the FlexARM project, which has received funding from the European Commission's Euratom Research and Training Programme 2014-2018 under the EUROfusion Engineering Grant EEG-2015/21 "Design of Control Systems for Remote Handling of Large Components".

REFERENCES

- [1] J. Burgner-Kahrs, D. C. Rucker, and H. Choset, "Continuum robots for medical applications: A survey," *IEEE Transactions on Robotics*, vol. 31, no. 6, pp. 1261–1280, 2015.
- [2] Y. Ganji, F. Janabi-Sharifi *et al.*, "Catheter kinematics for intracardiac navigation," *IEEE Transactions on Biomedical Engineering*, vol. 56, no. 3, pp. 621–632, 2009.
- [3] R. J. Webster III and B. A. Jones, "Design and kinematic modeling of constant curvature continuum robots: A review," *The International Journal of Robotics Research*, vol. 29, no. 13, pp. 1661–1683, 2010.
- [4] D. C. Rucker and R. J. Webster III, "Statics and dynamics of continuum robots with general tendon routing and external loading," *IEEE Transactions on Robotics*, vol. 27, no. 6, pp. 1033–1044, 2011.
- [5] T. Zheng, D. T. Branson, R. Kang, M. Cianchetti, E. Guglielmino, M. Follador, G. A. Medrano-Cerda, I. S. Godage, and D. G. Caldwell, "Dynamic continuum arm model for use with underwater robotic manipulators inspired by octopus vulgaris," in *2012 IEEE International Conference on Robotics and Automation*. IEEE, 2012, pp. 5289–5294.
- [6] F. Renda, M. Giorelli, M. Calisti, M. Cianchetti, and C. Laschi, "Dynamic model of a multibending soft robot arm driven by cables," *IEEE Transactions on Robotics*, vol. 30, no. 5, pp. 1109–1122, 2014.
- [7] S. Grazioso, V. Sonneville, G. Di Gironimo, O. Bauchau, and B. Siciliano, "A nonlinear finite element formalism for modelling flexible and soft manipulators," in *2016 IEEE International Conference on Simulation, Modeling, and Programming for Autonomous Robots*. IEEE, 2016, pp. 185–190.
- [8] S. Grazioso, G. Di Gironimo, and B. Siciliano, "A geometrically exact model for soft robots: the finite-element deformation space formulation," *IEEE Transactions on Robotics*, submitted.
- [9] S. S. Antman, *Nonlinear Problems of Elasticity*. Springer Science & Business Media, 2005, vol. 107.
- [10] J. C. Simo and L. Vu-Quoc, "A three-dimensional finite-strain rod model. part ii: Computational aspects," *Computer methods in applied mechanics and engineering*, vol. 58, no. 1, pp. 79–116, 1986.
- [11] V. Sonneville, A. Cardona, and O. Bruls, "Geometrically exact beam finite element formulated on the special euclidean group $se(3)$," *Computer Methods in Applied Mechanics and Engineering*, vol. 268, pp. 451–474, 2014.
- [12] F. Connolly, P. Polygerinos, C. J. Walsh, and K. Bertoldi, "Mechanical programming of soft actuators by varying fiber angle," *Soft Robotics*, vol. 2, no. 1, pp. 26–32, 2015.
- [13] F. Connolly, C. J. Walsh, and K. Bertoldi, "Automatic design of fiber-reinforced soft actuators for trajectory matching," *Proceedings of the National Academy of Sciences*, vol. 114, no. 1, pp. 51–56, 2017.
- [14] P. Maeder-York, T. Clites, E. Boggs, R. Neff, P. Polygerinos, D. Holland, L. Stirling, K. Galloway, C. Wee, and C. Walsh, "Biologically inspired soft robot for thumb rehabilitation," *Journal of Medical Devices*, vol. 8, no. 2, p. 020933, 2014.
- [15] P. Polygerinos, Z. Wang, K. C. Galloway, R. J. Wood, and C. J. Walsh, "Soft robotic glove for combined assistance and at-home rehabilitation," *Robotics and Autonomous Systems*, vol. 73, pp. 135–143, 2015.
- [16] K. M. Lynch and F. C. Park, *Modern Robotics: Mechanics, Planning, and Control*. Cambridge University Press, 2017.
- [17] S. Grazioso, G. Di Gironimo, and B. Siciliano, "From differential geometry of curves to helical kinematics of continuum robots using exponential mapping," in *Advances in Robot Kinematics 2018*. Springer, submitted.
- [18] F. Boyer and D. Primault, "Finite element of slender beams in finite transformations: a geometrically exact approach," *International Journal for Numerical Methods in Engineering*, vol. 59, no. 5, pp. 669–702, 2004.
- [19] E. Dowell and J. J. Traybar, "An experimental study of the nonlinear stiffness of a rotor blade undergoing flap, lag and twist deformations."